NOAA FORM 25-13 (1-78)

BIBLIOGRAPHIC DATA SHEET

U. S. DEPARTMENT OF COMMERCE
NATIONAL OCEANIC AND ATMOSPHERIC ADMINISTRATION

1. NOAA ACCESSION NUMBER	2.	3.
IDOE 79-112		PB80-129059

4. TITLE AND SUBTITLE	5. REPORT DATE
Geometry of the Subducted Lithosphere Beneath the Banda Sea in Eastern Indonesia from Seismicity and Fault Plane Solutions	June 1978
	6.
7. AUTHOR(S)	**8. REPORT NO.**
Richard K. Cardwell and Bryan L. Isacks	
9. PERFORMING ORGANIZATION NAME AND ADDRESS	**10. PROJECT/TASK NO.**
Cornell University, Ithaca, NY 14853, Department of Geological Sciences	**11. CONTRACT/GRANT NO.** IDE 75-21240
12. SPONSORING ORGANIZATION NAME AND ADDRESS	**13. TYPE OF REPORT AND PERIOD COVERED**
Office of the International Decade of Ocean Exploration National Science Foundation Washington, DC 20550	Reprint 14.

15. PUBLICATION REFERENCE

Reprinted from: Journal of Geophysical Research, Vol 83, no B6, p 2825-2838, June 10, 1978. 9 fig, 1 tab, 52 ref.

16. ABSTRACT The spatial distribution of hypocenters in eastern Indonesia, together with 41 new and previously published fault plane solutions, can be explained by a simple model of two lithospheric plates descending into the upper mantle beneath the Banda Sea. The major one, defined by the shallow to deep hypocenters located along the Banda arc, is a laterally continuous slab that has subducted at the plate coundary defined by the Java tranch-Timor trough-Aru trough system. The other slab descends toward the southwest to depths of about 100 km in the region of the Seram trough and may be joined to the Banda arc subduction system by the westward extension of the New Guinea Tarera-Aidoena fault zone, which acts as an arc-to-arc transform. The Banda arc slab is contorted at the eastern end of the arc where the trench and the line of active colcanoes curve to the northeast. The contortion appears to be a lateral bend in the subducted slab that is continuous from the surface to depths of 600 km. Fault plane solutions in the contorted portion of the slab have P axes aligned approximately parallel to the local strike of the slab and may be related to lateral bending stresses. Similar orientations of stress axes also occur near the curved ends of other island arcs. (Author modified)

17. KEY WORDS AND DOCUMENT ANALYSIS

17A. DESCRIPTORS

*Tectonics, *Lithosphere, Earthquakes, Seismology

17B. IDENTIFIERS/OPEN-ENDED TERMS

Eastern Indonesia, Banda Sea, International Decade of Ocean Exploration (IDOE)

17C. COSATI FIELD/GROUP

8K, 8G

18. AVAILABILITY STATEMENT	19. SECURITY CLASS (This report)	21. NO. OF PAGES
Released for distribution: Elaine S. Downs	UNCLASSIFIED	15 p.
	20. SECURITY CLASS (This report)	22. PRICE
	UNCLASSIFIED	

IDOE 79-112

VOL. 83, NO. B6 JOURNAL OF GEOPHYSICAL RESEARCH JUNE 10, 1978

Geometry of the Subducted Lithosphere Beneath the Banda Sea in Eastern Indonesia From Seismicity and Fault Plane Solutions

RICHARD K. CARDWELL AND BRYAN L. ISACKS

Department of Geological Sciences, Cornell University, Ithaca, New York 14853

The spatial distribution of hypocenters in eastern Indonesia, together with 41 new and previously published fault plane solutions, can be explained by a simple model of two lithospheric plates descending into the upper mantle beneath the Banda Sea. The major one, defined by the shallow to deep hypocenters located along the Banda arc, is a laterally continuous slab that has subducted at the plate boundary defined by the Java trench–Timor trough–Aru trough system. The other slab descends toward the southwest to depths of about 100 km in the region of the Seram trough and may be joined to the Banda arc subduction system by the westward extension of the New Guinea Tarera-Aidoena fault zone, which acts as an arc-to-arc transform. The Banda arc slab is contorted at the eastern end of the arc where the trench and the line of active volcanoes curve to the northeast. The contortion appears to be a lateral bend in the subducted slab that is continuous from the surface to depths of 600 km. Fault plane solutions in the contorted portion of the slab have *P* axes aligned approximately parallel to the local strike of the slab and may be related to lateral bending stresses. Similar orientations of stress axes also occur near the curved ends of other island arcs. Experiments with a lead sheet model suggest that the observed configuration of the Banda slab may be simply related to the curved end of the Banda arc and further suggest that the direction of relative motion between the Banda arc and Australia during the Neogene has been more north-northwesterly than the direction predicted from major plate motions. The discrepancy can be resolved if Southeast Asia is not considered part of the Eurasian plate. The lack of shallow underthrusting mechanisms and the paucity of shallow earthquakes in the Timor trough–Aru trough region may have resulted from the youthful collision of the Australian shelf with the Banda arc.

INTRODUCTION

Two of the most outstanding features of the eastern Indonesian region are the intensity of seismicity and the complexity of the presently active tectonic systems. The area includes the interaction of at least four major lithospheric plates: the Philippine, Indian-Australian, Pacific, and Eurasian plates. The nature of the interaction and the plate boundaries have yet to be clearly defined. Subduction dominates the present tectonic regime, major convergence occurring along the Philippine, New Guinea, and Java trenches. Moreover, the widespread distribution of mantle earthquakes and tectonic features characteristic of island arcs indicates the importance of subduction in the Neogene tectonic evolution of this region. Thus study of the highly active seismic zones and of the distribution and relationships of subducted slabs is essential to the understanding of both presently active and Neogene tectonics. In this study we focus on the boundary between eastern Indonesia and the Indian-Australian plate. We infer the shape of the descending slab from data on the distribution of earthquakes and focal mechanisms. With this information it is possible not only to determine the plate boundaries but also to infer information about the tectonic evolution of the region.

The Banda arc is the eastward continuation of the Sumatra-Java subduction system and has all the morphologic features that characterize many convergent plate margins, including a trench, trench slope break (nonvolcanic outer arc), upper slope basin, volcanic arc, and marginal basin (Figure 1). Interpretation of reflection profiles shows that the surface expression of subduction can be traced eastward from the Java trench to the Timor and Aru troughs [*Montecchi*, 1976; *Bowin et al.*, 1977; *Hamilton*, 1977*b*]. Reflection data reported in those references also indicate southward directed subduction beneath the Seram trough. The trench slope break is a submarine ridge (see the 1000-m contour in Figure 6) that is exposed at the outer arc islands of Timor, Jamdena, the Kai Islands, Seram, Buru, and many smaller islands and consists of complexes of subduction melange [*Hamilton*, 1977*b*]. The upper slope or forearc basins (Lombok, Savu, and Weber) consist of flat-lying sediments [*Hamilton*, 1977*b*] and are deeper than the Timor and Aru troughs, the Weber Basin being as deep as 7 km. From Java eastward the volcanic arc consists primarily of Neogene and Quaternary calc-alkaline volcanics. The Banda Basin, located on the concave side of the arc and floored by oceanic crust, is a marginal basin [*Bowin et al.*, 1977; *Purdy et al.*, 1977]. Although the Australian shelf appears to be colliding with and being subducted by the eastern Banda arc, the presence of the characteristic morphological features of subduction described above suggests that the collision is in a youthful stage.

Several papers by Audley-Charles and colleagues (for example, see *Audley-Charles* [1975]) present a view of the tectonics of the region based primarily on geological studies of Timor which is substantially different from the view presented above. However, we are convinced by the counterarguments of *Fitch and Hamilton* [1974] in this controversy and, like them, find the general picture described in the preceding paragraph most consistent with the seismological data.

One of the most striking aspects of the Banda arc is the apparent counterclockwise bend by about 180° at the eastern end. Because the morphologic features of the island arc appear continuous from Java to Buru, it has been suggested that the arc was at one time oriented east-west and has been bent counterclockwise into its present configuration by the northward movement of Australia and the westward movement of the Pacific [*Katili*, 1975]. A 180° bend of the slab can also be inferred from the hypocenter depth contours of *Hatherton and Dickinson* [1969] and *Hamilton* [1974*c*], although *Fitch and*

Paper number 8B0127.
0148-0227/78/068B-0127$01.00

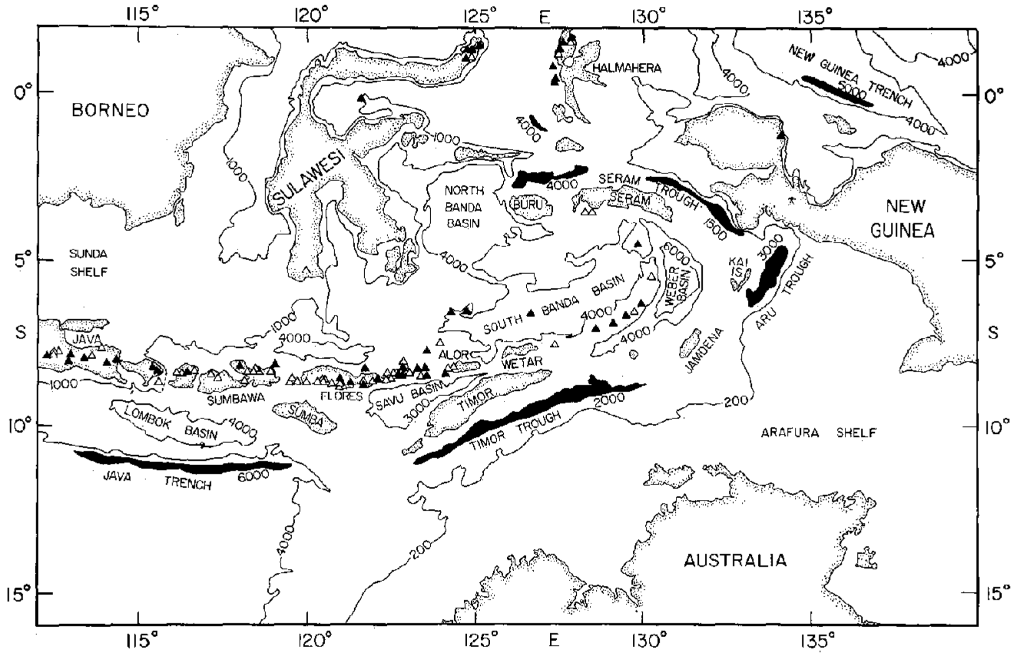

Fig. 1. Map of the Banda arc and eastern Indonesia. Bathymetry (in meters) is from *Hamilton* [1974*a*]. Historically active volcanoes from *Neumann van Padang* [1951] are shown as solid triangles; volcanoes of inferred Quaternary age are identified from Landsat imagery and are shown as open triangles.

Hamilton [1974] show only a 90° bend. Subduction around a 180° bend without disruption of the plate is difficult to imagine. We find instead that the data do not require a continuous subduction system from Java to Buru but are best explained by two subduction zones. One zone is along the Java trench–Timor trough–Aru trough system of the Banda arc, and another is along the Seram trough. In this interpretation the two are joined by the Tarera-Aidoena fault zone in western New Guinea, which acts as a transform fault. The Banda slab is inferred to have only a 90° bend at its eastern end.

Several previous studies have mainly used data recorded since 1961 and reported in the Preliminary Determination of Epicenters of the U.S. Geological Survey [*Hatherton and Dickinson,* 1969; *Fitch and Molnar,* 1970; *Fitch and Hamilton,* 1974; *Hamilton,* 1974*c*]. In order to cover a longer time period than that covered by previous studies, we examined, for the most part, the data reported in the *International Seismological Summary* (ISS) [*International Seismological Centre,* 1918–1963] and the *Bulletin of the International Seismological Centre* (ISC) [*International Seismological Centre,* 1964–1973] for over 50 years. To prevent contamination of the earthquake data file by poor quality events we carefully examined and graded each earthquake for the quality of its location. By selecting the best-located earthquakes we can achieve better resolution of the mantle seismic zones than existed before. The final data set consists of a large number of well-located earthquakes and is a substantial improvement over that used in previous studies.

Selection of Hypocenter Data

The sources of data used in this study are the ISS [*International Seismological Centre,* 1959–1963], the ISC [*International Seismological Centre,* 1964–1973], and the *Earthquake Data Report* (EDR) [*U.S. Geological Survey,* 1974 to April 1975]. In addition, all the well-located deep events reported in the ISS from 1918–1958 [*International Seismological Centre,* 1918–1958] are included in the data set.

Although this data set provides the most complete compilation of hypocenters covering the longest period of time available, it contains many imprecisely located events. We examined and graded the quality of each earthquake location with respect to the determination of depth by using data from local stations and *pP* readings and the determination of the epicenter by the azimuthal distribution of stations used in locating the event. Depth quality is judged from the number of consistent *pP* readings reported in the ISS, the ISC, and the EDR and from the number of stations with good residuals that are located at distances (Δ) of less than a certain function of the depth (h) of the event.

The following classification holds for intermediate (71- to 300-km) and deep events. A 'good' classification is assigned to an event with azimuthal coverage in three to four quadrants and with at least four to five consistent *pP* depth determinations and/or local stations with $h/\Delta \geq 0.7$. A 'fair' classification is assigned to an event with azimuthal coverage in at least three quadrants and with at least three consistent *pP* depth determinations and/or local stations with $h/\Delta \geq 0.2$. Events are rejected if there is azimuthal coverage in less than three quadrants or if there are no *pP* readings and no local stations with $h/\Delta \geq 0.2$.

For shallow events (0–70 km) the qualifications based on control of the depth are relaxed if there is still good control on the epicenter. The shallow depths will thus not be as well determined as the depths for the mantle events, but the locations will still provide high-quality data for map views of the distribution of epicenters.

In all cases the epicenter coordinates are taken from the ISS, the ISC, or the EDR, and the depth is determined from the reported *pP* readings. If no consistent *pP* readings are available, the depth given in the bulletin is used. The selection process has eliminated those earthquakes with poor locations caused by the lack of sufficient data controlling the hypocenter, but errors remain owing to the large velocity anomalies associated with subduction zones and to the effects of variations in the set of stations used for the locations. The errors in location may possibly increase the apparent thickness of the seismic zone, but the overall geometric configuration of the seismic zone described here will not be substantially affected. There may also be a systematic shift of locations in the upper 200 km due to effects of the velocity anomalies in the descending slab. Preliminary work in other regions indicates that this is not serious but could affect the precise relationships of the seismic zone to the surface features, such as volcanoes.

Figure 2 shows selected events located in the region of 2°–12°S, 115°–135°E. Since only teleseismic data were used, only events larger than about magnitude (m_b) 4.5 have been detected in their entirety. It is possible that some of the gaps in seismicity discussed below have small magnitude earthquakes that are not detected teleseismically. Even though 55% of the events were rejected by the selection process, the remaining events still adequately represent the spatial distribution of earthquakes because of the large number of data accumulated since the 1950's (for example, compare Figure 2 with the earthquake map of Southeast Asia [*National Earthquake Information Service*, 1970]. The few shallow and intermediate depth events located in western Sulawesi are not clearly related to the Banda arc and will not be discussed in this study.

In order to view the spatial distribution of earthquakes, vertical cross sections are made for the region. The width of each section is about 50 km, and the azimuth is approximately perpendicular to both the volcanic line and the trend of seismicity at constant depth. The trend of the trench is not used to align the sections because of the irregularities in the trend of the Banda arc. These irregularities are probably related to shallow deformational processes involved in the collision of the arc with the Australian shelf. The sections are then composited to make wider sections by matching common earthquakes that occur at the boundaries of adjacent sections, which, in the Banda arc, provide the best match between the overall distribution of events in adjacent sections. This result is a demonstration of the uniformity of deep structure along the strike of much of the Banda arc and agrees with similar results for other regions reported by *Isacks and Barazangi* [1977]. The azimuth and limits of the composite sections are shown in Figure 3, and the sections are shown in Figure 4.

SUBDUCTION ZONES IN EASTERN INDONESIA

The spatial distribution of intermediate and deep earthquakes defines the position of subducted lithospheric plates in the mantle. In Figure 2 it is clear that the zone of intermediate depth events is more or less continuous between Java and the north end of the Weber Basin and is approximately parallel to the trench and line of volcanoes, even where these features curve to the northeast at the eastern end of the arc. The zone of deep events is also laterally continuous and lies parallel to the line of volcanoes and trench, but it ends before the arc curves to the northeast.

Figure 4 shows that the inclined seismic zone along the entire Banda arc (sections A–F) is reasonably continuous with respect to depth. There is a seismic gap in section A from approximately 300 to 500 km, which, *Fitch and Molnar* [1970] note, extends west to the Sunda Strait. The gap in activity probably does not correspond to a gap in the lithosphere because the inclined zone appears continuous in the sections to the east (sections B–F and H). The inclined seismic zone in the mantle is well defined along the entire Banda arc and has a seismic thickness of about 30–40 km. The apparent seismic thickness is a combination of the real thickness, the effect of errors in location, and the effects of misprojection. The thickness observed here is close to the elastic thickness calculated for the bending of the suboceanic lithosphere [*Caldwell et al.*, 1976], although it is clearly less than the total lithospheric thickness of approximately 100 km.

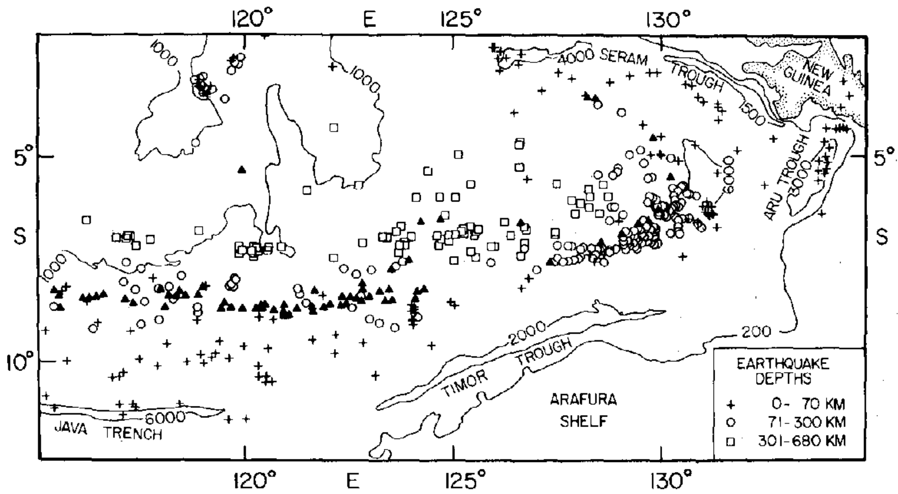

Fig. 2. Seismicity of the Banda arc region in eastern Indonesia (see text for data sources). All volcanoes in Figure 1 are shown here as solid triangles.

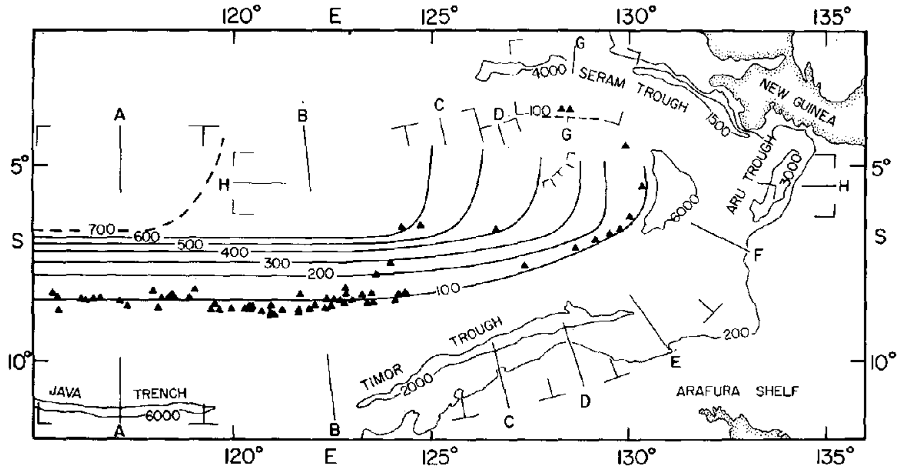

Fig. 3. Map showing depth contours (in kilometers) to the top of the inclined seismic zones in the Banda arc region of eastern Indonesia. Also shown are the locations and limits of the composite vertical cross sections which define the Banda arc subduction zone (sections A–F and H) and the Seram subduction zone (section G) shown in Figure 4. All volcanoes in Figure 1 are shown here as solid triangles. The extrapolated position of the 700-km contour is shown as a dashed line.

In sections B–E the seismic zone appears bent, the upper segment dipping more steeply than the lower one. The sharp bend in the downdip configuration is traceable and continuous from depths of 600 km (section B) upward and eastward to the bend in the Banda arc itself at its eastern end. This continuity of structure leads us to conclude that the deeper, flattened section is part of the slab subducted beneath the Banda arc and not a separate slab.

The dip of the upper 200 km of the seismic zone also becomes steeper toward the east. Past the region of maximum arc curvature the dip of the seismic zone rapidly decreases into a smoothly dipping zone (section F). The data suggest that the transition from section E to section F is continuous, and there is no evidence from either fault plane solutions or the spatial distribution of hypocenters to indicate a tear in this portion of the slab. Section H shows how the dipping zone of section F is continuous with the lower, flattened portion of the slab. The lower, flattened portion thus appears as a simple inclined zone that reaches the surface at the Aru trough.

The dashed lines in sections A–F are used along with map views of the distribution of hypocenters to construct a contour map of the top of the seismic zone. The resulting configuration of the top of the seismic zone shown in Figure 5 is the simplest one that fits the hypocentral data. Note how the contortion of the lower portion of the seismic zone manifests itself as a north-northeasterly bend in the slab contours and is continuous from the northeasterly bend in the trench to the zone of deep earthquakes. This subduction zone, which descends along the eastern Java trench–Timor trough–Aru trough system, will be referred to as the Banda arc subduction zone.

Where the Australian continental shelf collides with the Timor trough, there is no offset in the seismic zone, as can be seen by comparing sections A and B (the dashed line above the seismicity has the same shape for both sections in the upper 500 km). The lateral continuity of the subducted lithosphere from the Sunda arc (Java trench to the west) to the Banda arc argues against a major tectonic discontinuity between the arcs near Sumba as suggested by *Audley-Charles* [1975].

The Weber Basin does not appear to be a subduction zone trench as suggested by *Audley-Charles* [1975], because the mantle earthquakes beneath it (sections F and H) extend to the surface near the Aru trough. Morphologically, it appears to be an upper slope basin, and seismic reflection profiles show that it is filled with a thick sequence of flat-lying sediments [*Hamilton*, 1977*b*].

Although shallow focus earthquakes occur along the entire extent of the Java subduction zone, there are very few in the region between the Timor trough and the Aru trough. North of the Aru trough, along the Seram trough, the number of shallow focus earthquakes increases. The spatial distribution of earthquake hypocenters near the Seram trough is predominantly a shallow seismic zone dipping south to southwest to depths of about 100 km (section G). This inclined seismic zone, two new underthrusting mechanisms (see discussion in the next section), and reflection profiles [*Hamilton*, 1977*b*] indicate that subduction is occurring along the Seram trough.

There is a jump of over 100 km in the depth of the seismic zone between sections F and G. The paucity of intermediate depth events, the increase in shallow focus activity, and the change in dip of the seismic zone all suggest that the Seram trough subduction zone is not a continuation of the Banda arc subduction zone. This interpretation is supported by recent marine geophysical work which indicates that the Seram trough does not have continuity of structure with the Timor and Aru troughs [*Bowin et al.*, 1977]. The left lateral strike-slip Tarera-Aidoena fault zone in western New Guinea [*Visser and Hermes*, 1962] may act as a transform fault connecting the two subduction zones (Figure 5 (top)). The convergence along the Seram trough may become transferred to strike-slip motion along a zone that is related to the large left lateral strike-slip faults in Sulawesi, although at present the plate boundary is poorly defined.

The geometry of the subducted lithosphere and plate boundaries shown in Figure 5 differs in two important respects from results of previous studies [*Hatherton and Dickinson*, 1969; *Fitch and Molnar*, 1970; *Fitch and Hamilton*, 1974; *Hamilton*,

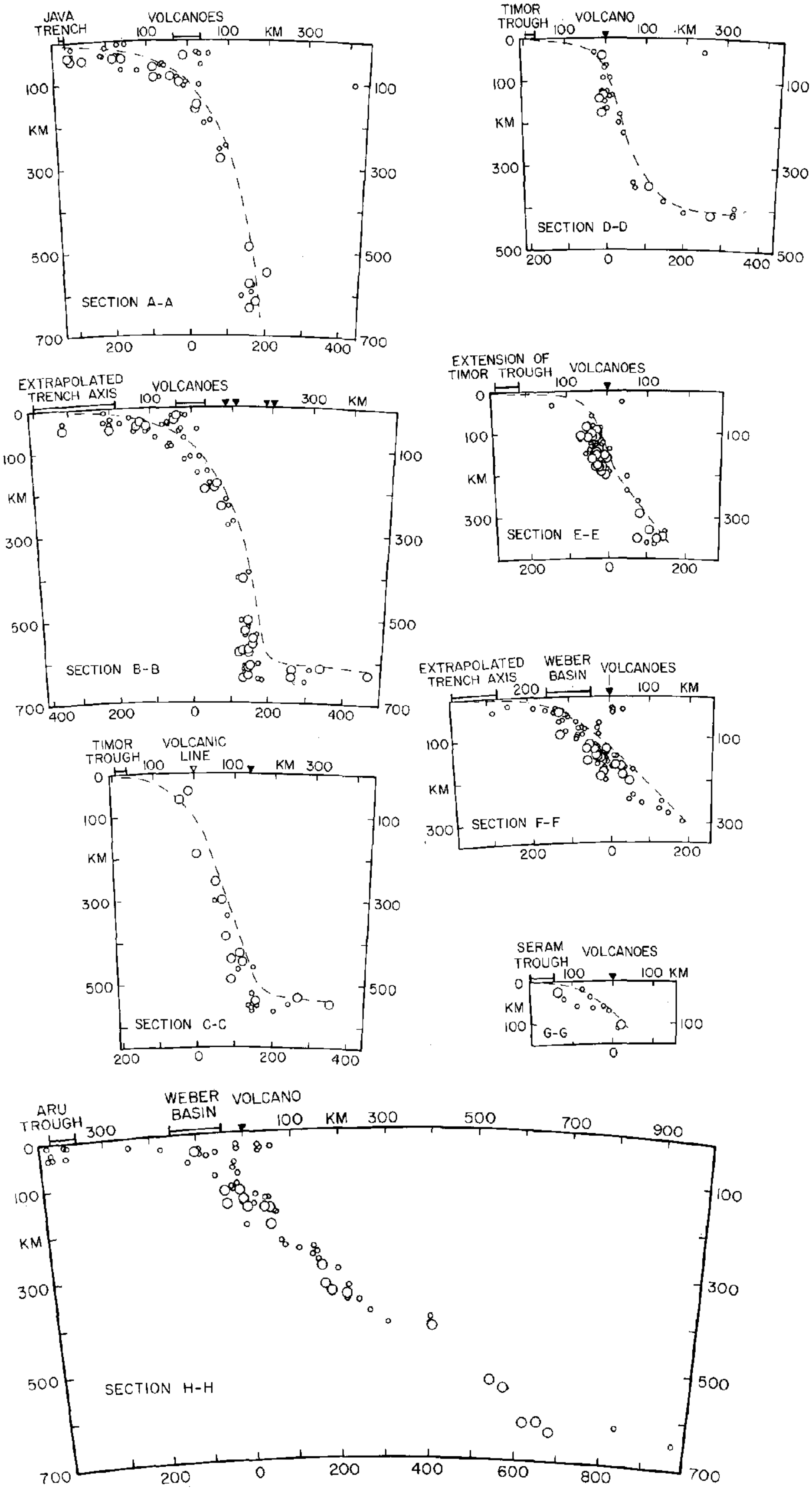

Fig. 4. Composite vertical cross sections of the earthquake hypocenters shown in Figure 2. Section locations and limits are shown in Figure 3. The range of variation of the projected position of the trench axis and the volcanoes in each section is shown by horizontal bars. Large circles represent locations that are better than those represented by the small circles (see text). The line above the seismic zone was used in constructing the contours of Figure 3. All sections have the same horizontal and vertical scales and include the earth's sphericity. The one isolated earthquake at 100 km in section A is part of the Sulawesi seismic zone and is not considered in this study. The volcanic line in section C is the extrapolated position of the main volcanic trend in sections B and D. The solid inverted triangles in sections B and C are volcanoes in the south Banda Basin.

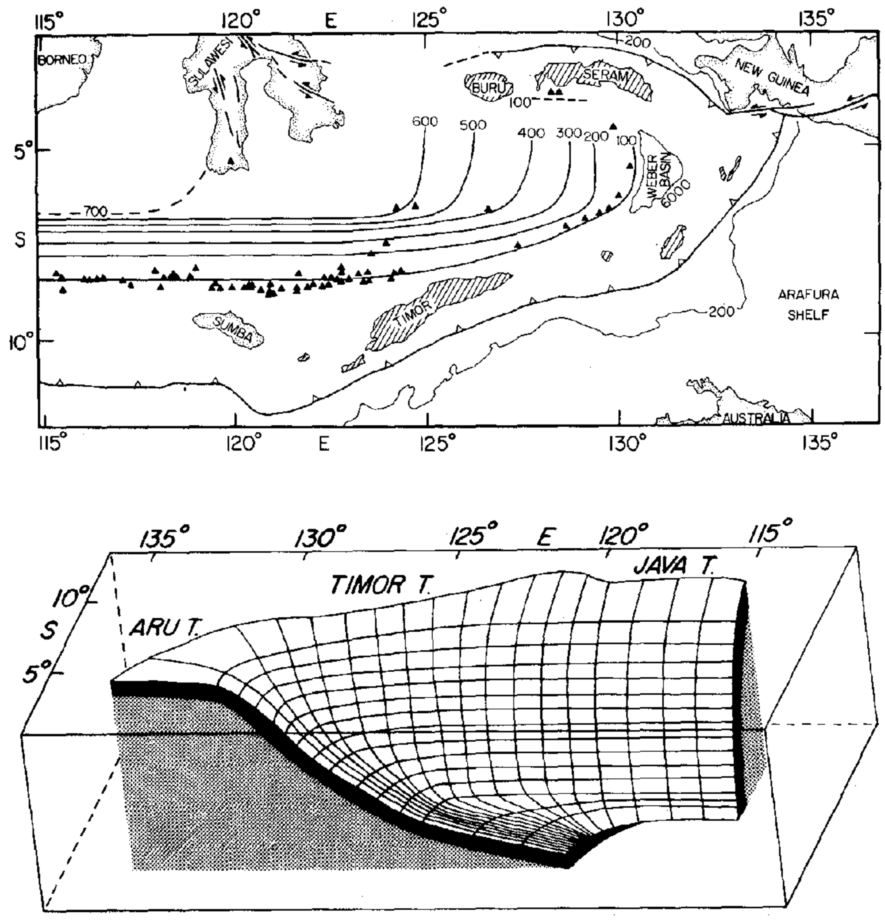

Fig. 5. (Top) Map showing major identified tectonic features and configuration of the subducted lithospheric slabs in the Banda arc region of eastern Indonesia. Contours of the top of the seismic zone are the same as in Figure 3. Large islands of the outer arc (the uplifted trench slope break) are hatchured. All volcanoes in Figure 1 are shown here as solid triangles. The surface expression of the Banda arc subduction zone (south of Timor) and the Seram trough subduction zone (north of Seram) is indicated by thrust fault symbols and is located along the trench axis by using the bathymetry from *Hamilton* [1974*a*]. The Tarera-Aidoena fault zone in western New Guinea and the faults in Sulawesi are from *Hamilton* [1974*c*]. The sense of motion of the fault zone in southwest Sulawesi is determined from Landsat imagery in this study. (Bottom) Block diagram illustrating the geometry of the subducted lithospheric slab in the Banda arc region of eastern Indonesia. The view is looking S17°E. Latitude and longitude are given for reference. The intersection of the slab with the surface is located near the back of the block and is given by the outline of the Java trench–Timor trough–Aru trough system. The configuration of the slab is given by a grid of two intersecting sets of curves. One set of curves lies in the horizontal plane at 50-km depth intervals from the surface (given by the trench outline) to a depth of 700 km. An additional curve has been added at 625 km for clarity. The other set of curves indicates the downdip orientation of the slab and is approximately orthogonal to the first set.

1974*a*, *b*, *c*]. The first difference is that the seismicity can be separated into two distinct subduction zones. The second difference is the downdip flattening of the seismic zone and the continuity of this feature from 600-km depths to the surficial bend of the arc. At the present time there is no seismic evidence for the occurrence of arc reversal north of Alor and Flores as suggested by *Hamilton* [1977*b*].

FAULT PLANE SOLUTIONS FOR SHALLOW EVENTS AND THE RELATIONSHIP TO SURFACE FEATURES

Eight new fault plane solutions for shallow earthquakes are combined with eight solutions published by *Fitch* [1970, 1972] in Figure 6. The data for these solutions and for the mantle events are illustrated in the appendix (Figure A1), and the parameters are given in Table 1. The majority of the mechanisms, whether of the thrusting (6–9 and 12–14) or strike-slip (10, 11, 15, and 16) type, are characterized by nearly horizontal compressional (*P*) axes. These mechanisms are consistent with the abundant geomorphological evidence for uplift of the Banda arc islands [*Van Bemmelen,* 1949; *Katili and Soetadi,* 1971; *Hamilton,* 1977*b*]. Except for two mechanisms on Sumba (8 and 9), most of the thrusting mechanisms have a large component of compression perpendicular to the arc and may reflect the collision of the Australian continental shelf with the arc.

The normal faulting mechanisms of events 1–3 may result from extensional bending stresses at the upper surface of the lithosphere as it subducts at the trench. New solutions 4 and 5 are the first mechanisms that can be interpreted as underthrusting at a subduction zone that have been found for the entire region east of the Sunda Strait. The two events are located along the Seram trough subduction zone. The inferred slip vectors trend west-southwest and indicate a component of oblique subduction.

No shallow underthrusting mechanisms have been found for the Banda arc subduction zone during the period 1961–1975. Since the beginning of this century there have been only two great shallow earthquakes along the Banda arc. One great earthquake occurred at the very end of the arc under the northern end of the Weber Basin (M_s = 8.2, February 1, 1938, 5.25°S, 130.5°E [*Gutenberg and Richter*, 1954]), and the other occurred recently along the Java trench (M_s = 7.75–8.0, August 19, 1977, 11.1°S, 118.4°E). The northernmost projection of the Australian continental shelf into the Timor trough–Aru trough subduction zone coincides with the region where very few shallow earthquakes occurred during the period 1959–1975 (Figure 2). Seismic refraction studies indicate that continental crust occurs beneath the sediments in the Timor and Aru troughs [*Bowin et al.*, 1977; *Shor et al.*, 1977]. On the basis of preliminary gravity modeling, *Chamalaun et al.* [1976] suggest that the Australian continental crust extends at least as far as the northern coast of Timor. The lack of underthrusting mechanisms and paucity of shallow earthquakes may thus be related to the subduction of the leading edge of the Australian continental shelf.

VOLCANOES

In general, the volcanoes are located about 100 km above the top of the seismic zone, in agreement with observations from other island arcs [*Isacks and Barazangi*, 1977]. The shallow earthquakes shown in sections A, B, D, F, and H above the seismic zone and below the volcanoes may be related to magmatic processes. Several studies [*Hatherton and Dickinson*, 1969; *Hutchison*, 1975, 1976; *Whitford*, 1975] have attempted to relate K, Sr, and Rb variation to the depth of the seismic zones by using the earthquake data of *Hatherton and Dickinson* [1969], *Fitch and Molnar* [1970], and *Hamilton* [1977*a*]. In map view the depth contours determined in this study (Figure 5 (top)) are systematically shifted away from the trench relative to the contours determined in the previous studies because we contoured the depth to the top of the seismic zone instead of the depths of earthquakes occurring within the slab. Therefore the top of the seismic zone represented by the contours in Figure 5 (top) is located at shallower depths below the volcanoes than that indicated by the contours determined previously.

It should be noted that five volcanoes lie off the main volcanic trend and are located above the deeper portions of the seismic zone. These include Batu Tara and three submarine volcanoes north of Alor (section B) and Api, north of Wetar (section C). The anomalous locations of these five volcanoes do not correspond to any major changes in the dip of the seismic zone. All five volcanoes occur near or within the south Banda Basin and may be a result of the occurrence of extensional tectonics within the marginal basin.

North of Sumba there appears to be a right lateral offset in the volcanic line (119°E), while south of Sumba there is a break in the continuity of the Java trench (Figure 6). *Audley-Charles* [1975] suggests that the arc is offset by a right lateral strike-slip fault that is a continuation of the fault zone in southwestern Sulawesi. Even though the volcanoes are slightly offset, there is no offset in the seismic zone, as can be seen by comparing sections A and B. In addition, our analysis of

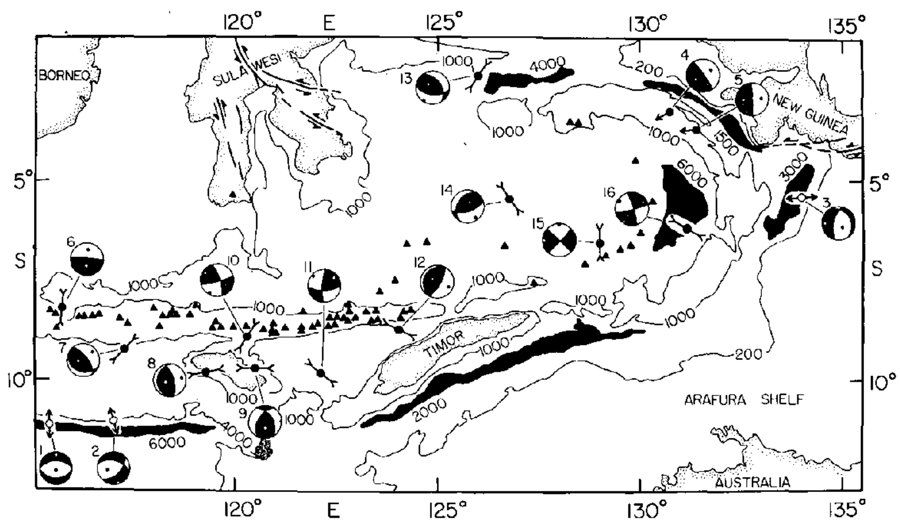

Fig. 6. Fault plane solutions for shallow earthquakes in the Banda arc of eastern Indonesia (see Table 1). Large circles are equal area projections of the lower hemispheres of the focal spheres. In each mechanism, solid quadrants represent compressional first motions, open quadrants represent dilatations, T axes are open circles, and P axes are solid circles. A small open circle with oppositely directed arrows shows the epicenter and the horizontal projection of the T axis for a normal fault solution (1, 2, and 3). A small solid circle with a single arrow shows the epicenter and the horizontal projection of the slip vector for an underthrusting solution (4 and 5). A small solid circle with opposing arrows shows the epicenter and the horizontal projection of the P axis for thrust fault (6–9 and 12–14) and strike-slip fault solutions (10, 11, 15 and 16). Bathymetry and fault zones are from *Hamilton* [1974*c*]. All volcanoes in Figure 1 are shown here as solid triangles.

TABLE 1. Fault Plane Solutions for Banda Arc Earthquakes

	Date	Position	Depth, km	Pole 1 Trend	Pole 1 Plunge	Pole 2 Trend	Pole 2 Plunge	*P* Axis Trend	*P* Axis Plunge	*T* Axis Trend	*T* Axis Plunge	*B* Axis Trend	*B* Axis Plunge	Reference*
1	March 30, 1967	11.14°S, 115.36°E	36	000	54	180	36	180	81	000	09	090	00	F13
2	May 28, 1972	11.05°S, 116.97°E	45	193	36	315	36	254	56	164	00	074	34	CI
3	April 23, 1964	5.42°S, 133.99°E	33	102	22	236	60	134	61	266	20	004	19	F24
4	Sept. 11, 1972	3.29°S, 130.75°E	37	238	05	058	85	058	40	238	50	328	00	CI
5	March 8, 1972	3.74°S, 131.39°E	29	267	05	087	85	087	40	267	50	257	00	CI
6	May 22, 1963	8.21°S, 115.69°E	56	186	06	006	84	006	39	186	51	96	00	F14
7	Jan. 9, 1970	9.27°S, 117.25°E	58	020	62	237	23	045	21	264	64	140	15	CI
8	April 10, 1973	9.81°S, 119.29°E	55	254	20	095	68	080	24	244	64	347	07	CI
9	March 24, 1963	9.70°S, 120.54°E	33	118	38	243	37	090	00	180	59	000	31	F12
10	Jan. 26, 1968	8.93°S, 120.32°E	29	254	14	355	07	210	05	301	14	102	75	F64
11	Nov. 5, 1972	9.82°S, 122.17°E	45	358	25	093	10	313	10	048	26	203	63	CI
12	June 28, 1970	8.75°S, 124.04°E	50	118	70	298	20	118	24	298	66	210	00	F63
13	Jan. 24, 1965	2.40°S, 125.98°E	6	011	35	237	45	213	07	310	64	120	25	F19
14	April 22, 1967	5.56°S, 126.81°E	33	122	53	353	30	146	12	026	66	240	21	F16
15	March 6, 1974	6.60°S, 128.98°E	26	046	00	316	08	001	06	270	06	136	82	CI
16	Sept. 24, 1972	6.22°S, 131.15°E	33	254	08	345	06	300	10	210	02	106	80	CI
17	Aug. 13, 1970	9.00°S, 117.95°E	99	323	23	118	65	135	21	340	66	228	10	CI
18	Feb. 14, 1963	7.19°S, 127.85°E	200	068	30	296	50	268	11	020	62	174	25	FM17
19	Sept. 29, 1969	7.27°S, 128.78°E	139	255	48	046	38	240	04	346	74	148	15	CI
20	Nov. 20, 1965	7.28°S, 129.16°E	122	142	60	272	20	110	22	241	59	010	22	FM16
21	July 8, 1971	7.03°S, 129.70°E	101	060	63	280	21	087	22	308	63	182	16	CI
22	Oct. 12, 1967	7.15°S, 129.83°E	86	240	30	355	36	029	02	296	49	122	41	F15
23	Sept. 5, 1972	6.95°S, 129.72°E	108	046	54	262	30	068	12	304	69	162	18	CI
24	Aug. 9, 1967	6.53°S, 130.53°E	91	226	36	358	44	023	04	284	64	114	25	FM13
25	May 12, 1965	6.20°S, 130.33°E	143	006	60	259	11	054	31	288	47	163	28	FM14
26	Feb. 24, 1969	6.23°S, 131.01°E	48	330	30	239	04	018	19	279	24	143	59	F62
27	Nov. 21, 1965	6.21°S, 130.39°E	125	149	60	266	15	104	24	235	52	003	25	FM12
28	Sept. 16, 1971	5.93°S, 130.68°E	125	112	05	292	85	112	50	292	40	021	00	CI
29	April 13, 1969	6.11°S, 129.91°E	163	184	54	004	36	184	09	004	81	274	00	CI
30	Aug. 8, 1969	6.14°S, 129.69°E	185	044	40	157	25	006	09	108	50	270	40	CI
31	July 8, 1964	5.54°S, 129.79°E	200	024	10	274	63	225	31	357	49	119	25	FM15
32	Aug. 20, 1965	5.74°S, 128.63°E	345	356	60	256	02	050	35	284	40	165	30	FM11
33	March 21, 1964	6.44°S, 127.96°E	351	088	48	355	04	033	35	144	24	258	43	TB
34	Feb. 11, 1969	6.76°S, 126.74°E	447	235	75	055	15	055	60	235	30	325	00	CI
35	Nov. 27, 1972	5.30°S, 126.62°E	419	354	26	096	23	046	36	315	02	223	54	CI
36	Aug. 4, 1969	5.71°S, 125.42°E	531	332	60	077	08	280	31	047	45	172	29	CI
37	April 4, 1972	7.47°S, 125.56°E	387	024	40	180	48	084	78	192	04	284	12	CI
38	June 22, 1966	7.21°S, 124.69°E	529	089	27	218	51	133	61	248	13	345	26	FM10
39	Oct. 18, 1964	7.17°S, 123.80°E	574	142	45	354	40	059	74	158	03	250	16	FM9
40	Nov. 9, 1967	7.18°S, 123.72°E	578	144	44	324	46	324	90	144	00	054	00	FM8
41	June 14, 1973	7.34°S, 120.32°E	639	332	30	128	58	002	72	143	14	237	11	CI

All hypocenters are selected by the method given in the text.

*The references are as follows: CI is this study, F is *Fitch* [1972], FM is *Fitch and Molnar* [1970], and TB is *Teng and Ben-Menahem* [1965]. The numbers after F and FM are those authors' original numbers for the earthquakes.

Landsat imagery, as well as the work of *Sukamto* [1975], suggests that the fault zone in southwestern Sulawesi is not right lateral but left lateral strike slip, as are many other faults in southern and central Sulawesi. At present, there is no evidence to show that a major right lateral strike-slip fault zone offsets the volcanic arc.

Fault Plane Solutions for Intermediate and Deep Events and Lateral Bending of the Slab

Twelve new fault plane solutions for mantle earthquakes are combined with twelve published by *Fitch and Molnar* [1970] and one by *Teng and Ben-Menahem* [1965] in Figure 7. For events 17–28 at intermediate depths the axes of minimum compressive stress (T axes) are oriented parallel to the dip of the seismic zone. This is in agreement with observations from other island arcs [*Isacks and Molnar*, 1971] that suggest that the descending slab is often under extension in this depth range. The configuration of the slab inferred from the distribution of hypocenters is supported by the change in the orientation of the T axes between mechanisms 18–23 and mechanisms 24–28. The T axes plunge in a northerly direction for mechanisms 18–23 and in a more westerly direction with smaller dip for mechanisms 24–28. Thus the T axes tend to follow the local dip of the slab.

Mechanisms 37–41 for deep focus events in the steeply dipping portion of the Banda arc subduction zone have axes of maximum compressive stress (P axes) oriented parallel to the dip of the seismic zone. Downdip compression is a well-known feature of many deep seismic zones [*Isacks and Molnar*, 1971]. Mechanism 36 for an event located near the end of the deep contorted seismic zone can also be interpreted as downdip compression.

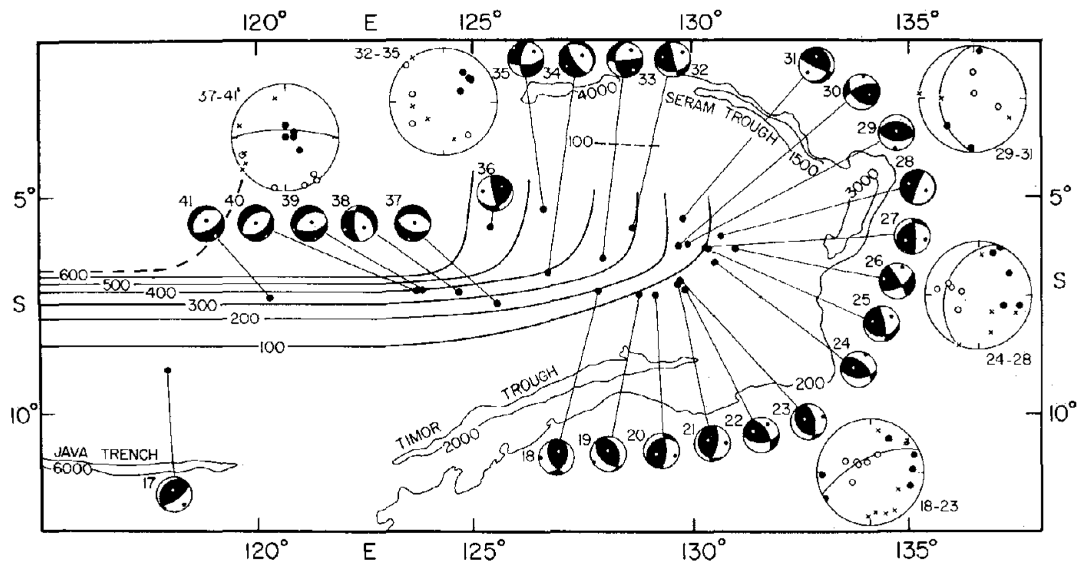

Fig. 7. Fault plane solutions for intermediate and deep earthquakes in the Banda arc region of eastern Indonesia (see Table 1). Mechanisms are represented as in Figure 6. A large focal sphere shows the orientation of P axes (solid circles), T axes (open circles), and B axes (crosses) for a group of mechanisms. The local orientation of the slab is shown on the large focal sphere except for events 32–35, which are located in a region of complex geometry. Contours of the top of the seismic zone (in kilometers) are the same as those in Figure 3.

Mechanisms 29–35 do not fit the simple pattern of downdip compression or tension. This might be expected, since the events occur in the most contorted portion of the slab. *Fitch and Molnar* [1970] noted that events 31, 32, and 33 have P axes approximately parallel to the local strike of the seismic zone and suggested that a lateral bending of the slab might give rise to compressional stresses parallel to the local strike of the slab. This type of stress distribution will be referred to as lateral compression.

New fault plane solutions for events 29, 30, 34, and 35 also have P axes aligned approximately parallel to the local strike of the seismic zone. Events 29–31 are closely grouped in a region where the slab dips to the west and strikes to the north, and for these events the P axes are oriented north-south. The deeper contorted portion of the slab has an average strike to the northeast. Even though the nodal planes of events 32–35 vary considerably among the mechanism solutions, the P axes are consistently aligned to the northeast.

In addition to the downdip orientation of the T axes, events 18–26 also have the P axes aligned parallel to the local strike of the slab. For events 18–23 the P axes trend northeasterly, and for events 24–26 they trend north-northeasterly. The combination of P axes parallel to the local strike of the slab and T axes oriented downdip for intermediate depth events 18–26 results in orientations of the B axes approximately perpendicular to the slab. These orientations are different from those of most planar seismic zones, in which the P or T axis is aligned downdip and the B axis is parallel to the seismic zone. However, mechanisms 27 and 28 both have the B axis in the more usual orientation parallel to the strike of the seismic zone.

Flexural bending of the slab is one mechanical model that might account for the observed stress distribution, since the subducted slab appears bent by about 90° at the eastern end of the arc. If bending is responsible for the stress distribution in the bent portion of the slab, then extensional stresses (T axes) as well as compressional stresses (P axes) should be aligned parallel to the local strike of the slab. Extensional stresses should develop on the convex side of the slab, and compressional stresses should develop on the concave side of the slab.

Isacks and Barazangi [1977] have noted that bending stresses may be important in the Peru and Kurile-Kamchatka subduction zones. In these cases the bending is not lateral but occurs about an axis parallel to the strike and could be interpreted as an elastic-plastic unbending effect. A similar interpretation could be applied to the results of *Umino and Hasegawa* [1975] for the northeast Japan arc. In all three cases, downdip compressional mechanisms occur near the top surface or convex side of the seismic zone, and downdip extensional mechanisms occur on the bottom or concave side of the zone.

In the eastern Banda arc, only lateral compressive stresses have been observed. The absence of mechanisms showing lateral extension may result from the existence of another stress system superimposed on the flexural bending stresses that reduces the magnitude of the extensional stresses. A stress distribution that would produce the desired result would consist of lateral compressive stresses that act in the plane of the plate and are nearly uniform throughout its thickness. Stresses of this general type are usually assumed in the interpretation of mantle earthquake mechanisms (i.e., *Isacks and Molnar* [1971]), although in those cases the orientations of the extensional and compressional axes are parallel to the dip of the slab rather than to its strike. Lateral stresses could arise as a consequence of deforming a section of a spherical shell of oceanic lithosphere as it subducts and assumes the plate configuration shown in Figures 3 and 4. The addition of a lateral compressive stress to the bending stresses would act to increase the magnitude of the lateral compressive stress but would reduce the magnitude of the lateral extensional stress on the other side of the plate.

This explanation, however, remains somewhat speculative. *Sasatani* [1976] also finds a predominance of laterally oriented compressive stress axes for the laterally bent portion of the slab descending beneath the Kurile-Hokkaido arc. The bend is located at depths greater than 200 km near the junction between the Kurile and north Honshu subduction zones. Sasatani also finds a predominance of vertical nodal planes approximately parallel to the axis of bending and suggests that the deformation takes place mainly along such a series of parallel faults. The Banda arc mechanisms, however, do not exhibit a pronounced regularity in the orientations of the nodal planes, and at present we remain inclined toward the thin plate elastic-plastic models of flexural bending.

A Simple Model of the Subducted Banda Arc Slab and Inferred Plate Motions

The contours in Figure 5 (top) are taken to represent the configuration of a segment of descending suboceanic lithosphere. The segment was presumably once part of a spherical shell on the surface, and in the process of subduction it has been bent downward and then deformed into its present shape. The dynamics of the process are not well understood. One can attempt to model certain geometrical aspects of the problem, however, if the deformation of the segment of the lithosphere is assumed to be done without significant areal strains. Our approach is to use a sheet of lead to model the lithospheric plate in order to investigate qualitatively two problems. The first one is to determine whether the configuration inferred in Figure 5 can be produced without significant areal strain or disruption of the lead sheet. This can be done with the lead sheet model, and therefore we find some support for the crude approximation that areal strains can be neglected. The second problem is to determine how the bend in the arc is related to the bend in the deeper portion of the descending slab. The continuity of the feature between the surface and 600 km suggests a close relationship. The lead sheet model suggests that the bend may be simply a result of subduction along an arc with a curved end. The interpretation of the Tarera-Aidoena fault zone as a transform fault is crucial to this model because it provides a free lateral edge to the subducted slab, which allows it to deform without tearing. We find that it is not possible to deform a single lead sheet into a continuous loop-shaped subduction zone extending from Java to Buru (as suggested in the model proposed by *Katili* [1975]) without tearing or substantially stretching the sheet.

We assume that the intersection of the subducted lithosphere with the earth's surface is along the Java trench–Timor trough–Aru trough system, and therefore we constrain the axis of downward bending of the lead sheet to a smoothed version of the trench outline. We use a lead sheet that is essentially inextensible for the range of deformation in the experiment. If the surface area of the lead sheet is not conserved and the sheet is allowed to stretch, then it would be possible to match the shape of any set of contours. The model includes the area from Java through the Aru trough at a scale of 1:3,000,000 and a thickness of the same order as the seismic thickness shown in Figure 4. For the qualitative experiment it is not crucial to model the lithosphere as 100-km thick or to include the effects of sphericity.

The procedure is to place the lead sheet on a wooden base which has a cutout of a smoothed version of the trench outline shown in Figure 5 (top). By bending the lead sheet over the 'trench' cutout it is possible to examine the configuration of a slab which is forced to subduct along a trench with a fixed outline. By bending the sheet over the trench cutout in successive increments, the development of the configuration in time can be simulated, and the effects of different subduction directions relative to the fixed 'trench' can be examined. This experiment, though crude, has provided valuable insight into what configurations are reasonable for a continuous, unbroken slab.

A major result of this simple experiment with the lead sheet is that it is possible to duplicate the shape shown by the contours in Figure 5 (top) without the need for any additional contortions or tears in the lead sheet. In order to conserve surface area and prevent tearing, it is observed that the dip of the lead sheet must steepen where the 'trench' begins to curve to the northeast (as in sections D and E of Figure 4). The lead sheet flattens out past the region of maximum 'trench' curvature (as in sections F and H of Figure 4) and dips gently to the west, forming the lower portion of the 'slab' (as seen in sections B–E of Figure 4). The contortion of the slab can therefore be simply a result of subduction at a trench where the curvature increases rapidly at one end. Away from the bend in the 'trench' the lead sheet is unaffected by the change in curvature and is not contorted (as in section A of Figure 4).

Thus the major features of the observed configuration of the Banda arc slab can be explained as a consequence of subduction at the curved eastern end of the arc. No special effect of the collision of Australia with the arc need be appealed to, which is in accordance with the hypothesis that the collision is in an early stage.

The geometry of the contorted slab must reflect the presently active tectonic system as well as the pattern of Neogene subduction. Experiments with the lead model suggest that the slab configuration may be a consequence of a north-northwesterly direction of convergence between the Banda arc and Australia. A north-northwesterly direction of convergence translates the contortion produced at the bend in the trench from the surface to depths of 600 km, as is observed in Figure 5. With a north-northwesterly direction of convergence there is a component of subduction perpendicular to the entire Banda arc which is consistent with the formation of the seven volcanoes at the far eastern end of the arc near the Weber Basin.

At the sharp bend in the arc near the Sunda Strait the earthquake depths shallow rapidly from over 600 km beneath Java to just over 200 km under Sumatra. *Fitch* [1970] could not account for all of the 400-km difference in depth using a north-northeasterly direction of convergence. A more north-northwesterly direction of convergence can account for more of the difference, since the Java trench near Sumatra will then be more parallel to the direction of subduction and will have only a small component of subduction perpendicular to the arc.

Along the entire boundary between Southeast Asia and the Indian-Australian plate there are only four reported underthrusting mechanisms [*Fitch,* 1972], all of which are located near Sumatra. One of these four events has a depth of 99 km (ISS), which if accurate would indicate that the mechanism probably represents downdip extensional stress in the slab instead of underthrusting. The same interpretation cannot be excluded for the other three events without further study of the depth of these events. The most recent pole determinations [*Minster et al.,* 1974] used no data from Asia and Indonesia because of the inadequate knowledge of the plate boundaries in this region. In the absence of abundant reliable slip vectors from shallow underthrusting mechanisms the distribution of volcanoes and the contortion of the slab discussed above may be the best indicators of the direction of relative movement between Asia and Australia. These data suggest a north-northwesterly convergence, at least until the continent-arc collision.

Various authors have suggested that a southeastward pushing of Southeast Asia toward Australia is reflected by the left lateral strike-slip motion along the Philippine fault zone and right lateral motions along the Barisan fault zone [*Vening Meinesz*, 1954; *Allen*, 1962; *Rodolfo*, 1969; *Katili*, 1970]. The recent work of *Molnar and Tapponnier* [1975] provides a mechanism for this direction of movement. Their model suggests that a large part of the convergence between the Indian subcontinent and Eurasia occurs by squeezing China eastward along major strike-slip faults. Southeast China and Southeast Asia are being translated to the southeast, as is indicated by the major strike-slip faults in Figure 8.

A relative motion between Southeast Asia and the Eurasian plate implies that Southeast Asia is not part of the Eurasian plate and that the pole of relative velocity determined by *Le Pichon et al.* [1973] for Eurasia and Australia should not be applied to the Banda arc. If Southeast Asia were rigidly attached to the Eurasian plate, then there would be a north-northeasterly direction of convergence between the Banda arc and Australia, which would be inconsistent with the evidence for north-northwest convergence determined above. Thus the difference between the convergence direction indicated in this study and that computed by assuming a rigid Eurasian plate also suggests that Southeast Asia is not part of the Eurasian plate. Further work is needed to define accurately the northern boundary of the proposed Southeast Asian plate.

LATERAL BENDING STRESSES VERSUS HINGE FAULTING AT THE ENDS OF ARCS

Several other island arcs in addition to the eastern Banda arc have a large curvature at one end of the arc. These include the northern Tonga arc, the southern New Hebrides arc, the northern West Indian and South Sandwich arcs, and the southern Marianas arc. Two of the arcs, the northern Tonga and South Sandwich arcs, have an extremely abrupt bend in the trench at the end of the arc and are characterized by hinge-faulting mechanisms at intermediate depths [*Isacks et al.*, 1969; *Forsyth*, 1975]. At the ends of the eastern Banda arc, the southern New Hebrides arc, and the southern Marianas arc, the trench has a smaller curvature than it has in the northern Tonga or South Sandwich arcs. In addition, fault plane solutions for earthquakes located near the ends of the three more gently curved arcs are indicative of lateral compression and/or lateral extension for intermediate depth earthquakes. There

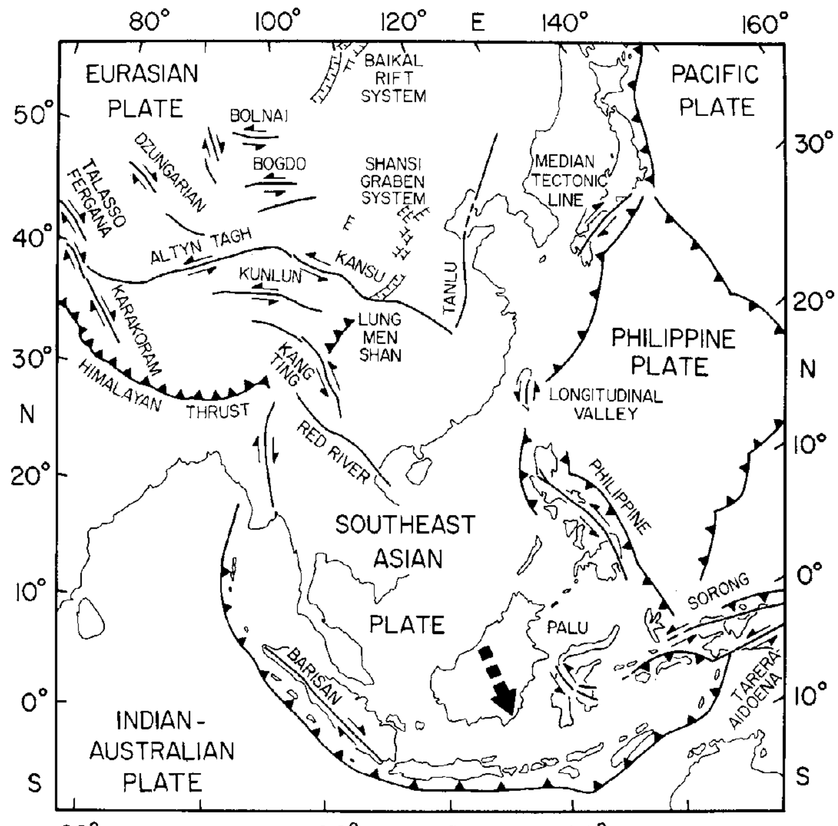

Fig. 8. Major well-established faults and subduction zones of Southeast Asia. Indonesian faults are taken from *Hamilton* [1974c], Philippine and Longitudinal Valley faults from *Allen* [1962], Median Tectonic Line from *Kaneko* [1966] and *Okada* [1971], and faults in China from *Molnar and Tapponnier* [1975] and *York et al.* [1976]. The large dashed arrow indicates the approximate direction of convergence between Australia and the Banda arc determined in this study. The convergence direction determined from this study is different from that calculated from major plate motions and suggests that Southeast Asia may act as an independent plate. The northern boundary of the proposed Southeast Asian plate is not clearly defined.

are no mechanisms for intermediate depth earthquakes at the bend of the northern West Indian arc, but the trench curvature best matches the curvatures found in the gently curved group. In addition, the work of *Molnar and Sykes* [1969, 1971] suggests that hinge faulting is not occurring at the northern end of the West Indian arc.

Three fault plane solutions have been published for intermediate depth earthquakes in the southern New Hebrides region where the trench bends to the east [*Isacks and Molnar,* 1971]. Two mechanisms can be interpreted as lateral extension, and one as lateral compression. The otherwise puzzling variation between the orientation of these three mechanisms can thus be explained as a lateral bending effect if the event indicative of lateral compression is on the side of the slab opposite the two events indicative of lateral extension. Further analysis of these locations is required to resolve this question.

There is only one mechanism for the curved zone of intermediate depth earthquakes in the Marianas island arc [*Isacks and Molnar,* 1971]. The mechanism is best interpreted as showing lateral extension.

Although the subducted slabs appear to bend at the ends of the southern Marianas and New Hebrides arcs, it is not clearly understood how these arcs terminate past the bend. In the Banda arc, however, the subducted slab appears to be terminated along a transform fault (Figure 5). Since the transform fault extends from the convex side of the arc, no hinge faulting occurs at the end of the Banda arc. This allows the free edge of the Banda arc slab to subduct and deform without difficulty.

The zone of intermediate depth earthquakes and the trench axis both bend very abruptly at the northern end of the South Sandwich arc. Hinge-faulting mechanisms and downdip extensional mechanisms occur for intermediate depth events near the bend in the trench [*Isacks and Molnar,* 1971; *Forsyth,* 1975]. There is no evidence to support lateral bending stresses as are found in the arcs with more gentle curvature discussed above. At the northern edge of the South Sandwich arc the lithosphere is torn along a nearly vertical fault zone as it subducts near the bend in the trench instead of contorting as it does in the eastern Banda arc.

The Tonga arc appears to be a special and interesting case. *Fitch and Molnar* [1970] compared the northern end of Tonga to the Banda arc and suggested that both are cases in which the slab terminates along a bent edge. Further resolution of the Tonga structure [*Isacks and Barazangi,* 1977], however, shows that the upper 400 km of the north Tonga slab is not bent very much laterally. The termination of the arc by a hinge fault does not require any bending of the subducted plate. Moreover, the bend in the trench is quite abrupt, in contrast to the more gentle bending at the eastern end of the Banda arc. In addition, the line of Tonga calc-alkaline volcanoes does not bend around as does the line of volcanoes in the Banda arc. Thus the present termination of the northern Tonga arc is quite different from that proposed for the Banda arc.

However, the remarkable contortion of the Tonga slab below 400 km may be interpreted as a result of a previous episode of subduction which may be more similar to that now operating in the Banda arc. The northern end of the Tonga deep zone is sharply bent around to the west. Plate reconstructions for the Tonga-Fiji region [*Chase,* 1971; *Gill and Gorton,* 1973] plus the distribution of deep earthquakes beneath the New Hebrides–Fiji Plateau–Tonga region indicate that prior to about 10 m.y. ago, Pacific lithosphere was subducted southwestward along an extensive arc system connecting the Tonga arc with an extinct system trending northwest from the northern Tonga arc to the Solomons. The contortion at the northern end of the Tonga deep zone thus may be a remnant of subduction around a bend in the old arc system. The contortion in the Banda slab is also thought to have developed by subducting at a curved end of the trench (see discussion in the previous section). Later, as the subduction direction became more westerly in the Tonga region, a planar seismic zone with hinge faulting developed.

CONCLUSIONS

A detailed study of the spatial distribution of carefully selected hypocenters and fault plane solutions in eastern Indonesia shows that the data can be explained by a simple model in which two lithospheric plates descend beneath the Banda Sea. The major one descends toward the north beneath the Banda arc. The second one probably descends toward the southwest in the region of Seram and may be joined to the Banda arc system by the Tarera-Aidoena fault zone in western New Guinea, which acts as an arc-to-arc transform fault.

The slab beneath the eastern Banda arc is contorted because it subducted at the end of an arc where the trench bends to the northeast. Fault plane solutions in the contorted portion of the subducted slab indicate that the slab is undergoing a lateral compression, which may be caused by bending. Lateral bending stresses are also observed in the southern New Hebrides and Marianas arcs, where the trench bends gently at one end of the arc. Away from the contorted portion of the Banda arc slab the stresses are oriented in the more usual downdip configuration.

The continuity of the elements of the arc around the bend and the propagation of the bend down the slab to depths of 600 km suggest that the convergence between the Indian-Australian plate and Southeast Asia in the vicinity of the Banda Sea has been in a north-northwest direction, at least until the continent-arc collision. This convergence direction is different from that determined by using the pole of rotation between the Indian-Australian and the Eurasian plates and indicates that Southeast Asia may be a separate plate from the Eurasian plate.

The lack of underthrusting fault plane solutions along the Java trench–Timor trough–Aru trough system and the paucity of shallow earthquakes are consistent with the subduction of the leading edge of the Australian continental shelf.

APPENDIX

Table 1 lists the solution parameters for all fault plane solutions in the Banda arc region of eastern Indonesia obtained by using the long-period seismographs of the World Wide Network of Standardized Seismographs. The 20 new solutions ('CI' in Table 1) are illustrated in the appendix on equal area projections of the lower hemisphere of the focal sphere. Large and small open circles represent clear and uncertain dilatational first motions, respectively. Large and small solid circles represent clear and uncertain compressional first motions, respectively. Large and small crosses indicate clear and uncertain compressional wave data judged to be near a nodal plane, respectively. Open and solid boxes represent clear and uncertain *pP* motions projected through the center onto the lower hemisphere of the focal sphere, respectively. Arrows indicate *S* wave polarization directions. Tick marks on the nodal planes indicate the poles to the planes. The *P* and *T* axes are located at the base of the letters *P* and *T*. The symbols below the focal sphere give the date, latitude, longitude, and depth of the mechanism.

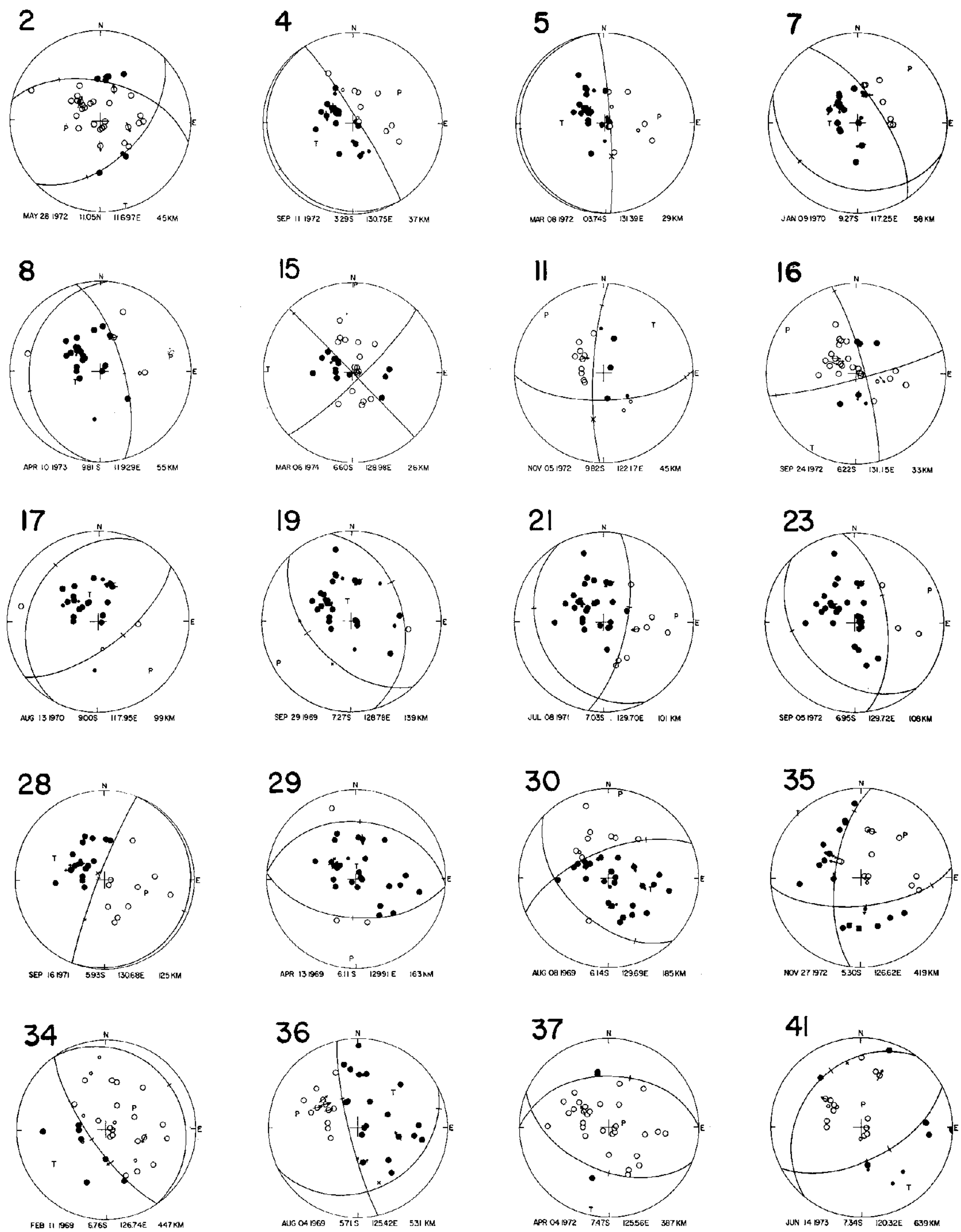

Fig. A1. New focal mechanism solutions determined by this study for the earthquakes listed in Table 1.

Acknowledgments. We thank Muawia Barazangi and Jack Oliver for useful discussions and for carefully reviewing this paper, and we thank S. Billington, A. DeRamos, J. Chiu, N. Fitzpatrick, D. Friedman, J. Ni, and J. York for assistance on different aspects of this paper. This work is supported by National Science Foundation grant IDE 75-21240. Contribution 610 of the Department of Geological Sciences at Cornell University.

REFERENCES

Allen, C., Circum-Pacific faulting in the Philippines-Taiwan region, *J. Geophys. Res.*, *67*, 4795–4812, 1962.

Audley-Charles, M. G., The Sumba fracture: A major discontinuity between eastern and western Indonesia, *Tectonophysics*, *26*, 213–228, 1975.

Bowin, C. O., G. M. Purdy, G. Shor, L. Lawver, H. M. S. Hartono, C. Johnston, F. Chamalaun, and J. Sunderland, Geophysical study of the Banda Arc, Indonesia (abstract), *Eos Trans. AGU*, *58*, 509, 1977.

Caldwell, J. G., W. F. Haxby, D. E. Karig, and D. L. Turcotte, On the applicability of a universal elastic trench profile, *Earth Planet. Sci. Lett.*, *31*, 239–246, 1976.

Chamalaun, F. H., K. Lockwood, and A. White, The Bouguer gravity field and crustal structure of eastern Timor, *Tectonophysics*, *30*, 241–259, 1976.

Chase, C. G., Tectonic history of the Fiji Plateau, *Geol. Soc. Amer. Bull.*, *82*, 3087–3110, 1971.

Fitch, T. J., Earthquake mechanisms and island arc tectonics in the Indonesian-Philippine region, *Bull. Seismol. Soc. Amer.*, *60*, 565–591, 1970.

Fitch, T. J., Plate convergence, transcurrent faults, and internal deformation adjacent to Southeast Asia and the western Pacific, *J. Geophys. Res.*, *77*, 4432–4460, 1972.

Fitch, T. J., and W. Hamilton, Reply, *J. Geophys. Res.*, *79*, 4982–4985, 1974.

Fitch, T. J., and P. Molnar, Focal mechanisms along inclined earthquake zones in the Indonesian-Philippine region, *J. Geophys. Res.*, *75*, 1431–1444, 1970.

Forsyth, D. W., Fault plane solutions and tectonics of the South Atlantic and Scotia Sea, *J. Geophys. Res.*, *80*, 1429–1443, 1975.

Gill, J., and M. Gorton, A proposed geological and geochemical history of eastern Melanesia, in *The Western Pacific: Island Arcs, Marginal Seas, Geochemistry*, edited by P. J. Coleman, pp. 543–566, University of Western Australia Press, Nedlands, Australia, 1973.

Gutenberg, B., and C. F. Richter, *Seismicity of the Earth and Associated Phenomena*, 310 pp., Princeton University Press, Princeton, N. J., 1954.

Hamilton, W., Bathymetric map of the Indonesian region, scale 1:5,000,000, *Misc. Invest. Ser., Map I-875-A*, U.S. Geol. Surv., Reston, Va., 1974*a*.

Hamilton, W., Map of sedimentary basins of the Indonesian region, scale 1:5,000,000, *Misc. Invest. Ser., Map I-875-B*, U.S. Geol. Surv., Reston, Va., 1974*b*.

Hamilton, W., Earthquake map of the Indonesian region, scale 1:5,000,000, *Misc. Invest. Ser., Map I-875-C*, U.S. Geol. Surv., Reston, Va., 1974*c*.

Hamilton, W., Tectonic map of the Indonesian region, scale 1:5,000,000, *Misc. Invest. Ser., Map I-875-D*, U.S. Geol. Surv., Reston, Va., 1977*a*.

Hamilton, W., Subduction in the Indonesian region, in *Island Arcs, Deep Sea Trenches, and Back-Arc Basins, Maurice Ewing Ser.*, vol. 1, edited by M. Talwani and W. C. Pitman III, pp. 15–31, AGU, Washington, D. C., 1977*b*.

Hatherton, T., and W. R. Dickinson, The relationship between andesitic volcanism and seismicity in Indonesia, the Lesser Antilles, and other island arcs, *J. Geophys. Res.*, *74*, 5301–5310, 1969.

Hutchison, C. S., Correlation of Indonesian active volcanic geochemistry with Benioff zone depth, *Geol. Mijnbouw*, *54*, 157–168, 1975.

Hutchison, C. S., Indonesian active volcanic arc: K, Sr, and Rb variation with depth to the Benioff zone, *Geology*, *4*, 407–408, 1976.

International Seismological Centre, *International Seismological Summary*, Newbury, Berkshire, U.K., 1918–1963.

International Seismological Centre, *Bulletin of the International Seismological Centre*, Newbury, Berkshire, U.K., 1964–1973.

Isacks, B. L., and M. Barazangi, Geometry of Benioff zones: Lateral segmentation and downwards bending of the subducted lithosphere, in *Island Arcs, Deep Sea Trenches, and Back-Arc Basins, Maurice Ewing Ser.*, vol. 1, edited by M. Talwani and W. C. Pitman III, pp. 99–114, AGU, Washington, D. C., 1977.

Isacks, B., and P. Molnar, Distribution of stress in the descending lithosphere from a global survey of focal mechanism solutions of mantle earthquakes, *Rev. Geophys. Space Phys.*, *9*, 103–174, 1971.

Isacks, B., L. Sykes, and J. Oliver, Focal mechanisms of deep and shallow earthquakes in the Tonga-Kermadec region and the tectonics of island arcs, *Geol. Soc. Amer. Bull.*, *80*, 1443–1470, 1969.

Kaneko, S., Transcurrent displacement along the median line, southwestern Japan, *N. Z. J. Geol. Geophys.*, *2*, 45–59, 1966.

Katili, J. A., Large transcurrent faults in Southeast Asia with special reference to Indonesia, *Geol. Rundsch.*, *59*, 581–600, 1970.

Katili, J. A., Volcanism and plate tectonics in the Indonesian island arcs, *Tectonophysics*, *26*, 165–188, 1975.

Katili, J. A., and R. Soetadi, Neotectonics and seismic zones of the Indonesian Archipelago, *Proc. Roy. Soc. N. Z.*, *9*, 39–45, 1971.

Le Pichon, X., J. Francheteau, and J. Bonnin, *Plate Tectonics*, p. 85, Elsevier, New York, 1973.

Minster, J. B., T. H. Jordan, P. Molnar, and E. Haines, Numerical modeling of instantaneous plate tectonics, *Geophys. J. Roy. Astron. Soc.*, *36*, 541–576, 1974.

Molnar, P., and L. Sykes, Tectonics of the Caribbean and Middle America regions from focal mechanisms and seismicity, *Geol. Soc. Amer. Bull.*, *80*, 1639–1684, 1969.

Molnar, P., and L. Sykes, Plate tectonics in the Hispanola area: Discussion, *Geol. Soc. Amer. Bull.*, *82*, 1123–1126, 1971.

Molnar, P., and P. Tapponnier, Tectonics of Asia: Consequences and implications of a continental collision, *Science*, *189*, 419–426, 1975.

Montecchi, P. A., Some shallow tectonic consequences of 'subduction' and their meaning to the hydrocarbon explorationist, in *Circum-Pacific Energy and Mineral Resources, Mem. 25*, edited by M. T. Halbouty, J. C. Maher, and H. M. Lian, American Association of Petroleum Geologists, Tulsa, Okla., 1976.

National Earthquake Information Service, Seismicity of Southeast Asia, *Map NEIC-3009*, Nat. Ocean Surv., Nat. Oceanic and Atmos. Admin., Riverdale, Md., 1970.

Neumann van Padang, M., *Catalogue of the Active Volcanoes of the World Including Solfatara Fields*, part 1, *Indonesia*, International Volcanological Association, Naples, 1951.

Okada, A., Active faulting of the median tectonic line (in Japanese), *Kagaku Tokyo*, *41*, 666–669, 1971.

Purdy, G. M., R. Detrick, and G. G. Shor, Crustal structure of the Banda Sea and Weber Deep (abstract), *Eos Trans. AGU*, *58*, 509, 1977.

Rodolfo, K. S., Bathymetry and marine geology of the Andaman Basin, and tectonic implications for Southeast Asia, *Geol. Soc. Amer. Bull.*, *80*, 1203–1230, 1969.

Sasatani, T., Mechanism of mantle earthquakes near the junction of the Kurile and the northern Honshu arcs, *J. Phys. Earth*, *24*, 341–354, 1976.

Shor, G. G., R. S. Jacobson, and G. M. Purdy, Structure beneath the Timor-Tanimbar-Aru trough system (abstract), *Eos Trans. AGU*, *58*, 509, 1977.

Sukamto, R., The structure of Sulawesi in the light of plate tectonics, paper presented at Regional Conference on the Geology and Mineral Resources of Southeast Asia, Ass. of Indones. Geol., Jakarta, Aug. 4–7, 1975.

Teng, T., and A. Ben-Menahem, Mechanism of deep earthquakes from spectrums of isolated body wave signals, *J. Geophys. Res.*, *70*, 5157–5170, 1965.

Umino, N., and A. Hasegawa, On the two layer structure of deep seismic plane in northeast Japan arc (in Japanese), *J. Seismol. Soc. Jap., Ser. 2*, *28*, 125–139, 1975.

U.S. Geol. Surv., *Earthquake Data Report*, Arlington, Va., 1974 to April 1975.

Van Bemmelen, R. W., *The Geology of Indonesia*, 732 pp., Government Printing Office, The Hague, 1949.

Vening Meinesz, F. A., Indonesian Archipelago: A geophysical study, *Geol. Soc. Amer. Bull.*, *65*, 143–164, 1954.

Visser, W. A., and J. J. Hermes, Geological results of the exploration for oil in Netherlands New Guinea, *Verh. Kon. Ned. Geol. Mijnbouwk. Genoot. Geol. Ser.*, *20*, 1–265, 1962.

Whitford, D. J., Strontium isotopic studies of the volcanic rocks of the Sunda arc, Indonesia, and their petrogenetic implications, *Geochim. Cosmochim. Acta*, *39*, 1287–1302, 1975.

York, J. E., R. Cardwell, and J. Ni, Seismicity and Quaternary faulting in China, *Bull. Seismol. Soc. Amer.*, *66*, 1983–2001, 1976.

(Received June 27, 1977;
revised November 23, 1977;
accepted January 23, 1978.)